Biogeosciences Discuss., 6, 8075–8100, 2009
www.biogeosciences-discuss.net/6/8075/2009/

Biogeosciences Discussions

Biogeosciences Discussions is the access reviewed discussion forum of *Biogeosciences*

Optical characterization of an eddy-induced diatom bloom west of the island of Hawaii

F. Nencioli[1], **G. Chang**[2], **M. Twardowski**[3], **and T. D. Dickey**[1]

[1]Ocean Physics Laboratory, Department of Geography, University of California, Santa Barbara, CA 93106, USA
[2]Sea Engineering Inc., 200 Washington St. Suite 210, Santa Cruz, CA 95060, USA
[3]Dept. of Research, WET Labs Inc., Narragansett, RI, 02882, USA

Received: 2 July 2009 – Accepted: 20 July 2009 – Published: 7 August 2009

Correspondence to: F. Nencioli (francesco.nencioli@opl.ucsb.edu)

Published by Copernicus Publications on behalf of the European Geosciences Union.

Abstract

Optical properties are used to characterize the biogeochemistry of cyclonic eddy *Opal* in the lee of Hawaii. The eddy featured an intense diatom bloom. Our results show that the ratio of chlorophyll concentration to particulate beam attenuation coefficient, [chl]/c_p, is not a good indicator of the changes in particle composition through the water column. The ratio is controlled primarily by the variation in chlorophyll concentration per cell with depth (photoadaptation), so that its values increase throughout the Deep Chlorophyll Maximum Layer (DCML). Below the DCML, high values of [chl]/c_p suggest that remineralization might be another important controlling factor. On the other hand, the backscattering ratio (particle backscattering to particle scattering ratio, $\tilde{b}_{bp}$) clearly indicates a shift from a small phytoplankton to a diatom dominated community. Below an upper layer characterized by constant values, the $\tilde{b}_{bp}$ ratio showed a rapid decrease to a broad minimum within the DCML. The higher values below the DCML are consistent with enhanced remineralization below the eddy-induced bloom. The DCML was characterized by a layer of "healthy" diatoms underlying a layer of "senescent" diatoms. These two layers are characterized by similar optical properties, indicating some possible limitations in using optical measurements to fully characterize the composition of suspended material in the water column. An inverse relationship between $\tilde{b}_{bp}$ and [chl]/c_p, also reported by others, is observed as deep as the DCML. There, [chl]/c_p increases whereas $\tilde{b}_{bp}$ remains similar to values found in the empty frustule layer. This is a further indication that [chl]/c_p might not be a good alternative to the backscattering ratio for investigating changes in particle composition with depth in Case I waters.

1 Introduction

In the last two decades, many studies have focused on the relationships between optical properties and biogeochemical constituents (e.g., phytoplankton, sediment, dissolved matter) in order to develop rapid, continuous, in situ techniques for retrieving

BGD

6, 8075–8100, 2009

information such as the amount, type and composition of suspended material in the water column. Several optical parameters can now be used to obtain information on ocean living and non-living particles, both from in situ and remote sensing platforms. Chlorophyll fluorescence, beam attenuation coefficient (c_p, m^{-1}), total particulate scattering (b_p, m^{-1}), particulate backscattering (b_{bp}, m^{-1}), and slope of the spectral attenuation coefficient (γ) are the optical quantities of interest in this study.

Chlorophyll fluorescence and c_p have long been used to measure, respectively, total chlorophyll and total particulate organic carbon (POC) concentrations in open ocean (Case I) waters (Morel, 1988; Siegel et al., 1989). The coefficients, b_{bp} and b_p, can be used to obtain information on the composition of particulate material. For example, Twardowski et al. (2001) showed that the backscattering ratio (b_{bp}/b_p, herein $\tilde{b}_{bp}$) can be used as a proxy for the bulk refractive index of particles, which depends on the bulk particulate composition. Particle assemblages dominated by inorganic material are generally characterized by higher values of bulk refractive index, and thus higher values of $\tilde{b}_{bp}$, whereas assemblages dominated by organic particles such as phytoplankton and dead cell material are characterized by lower values. The slope of spectral c_p, γ, can be used to estimate the particle size distribution (PSD) slope (ξ) through the relationship $\gamma \approx \xi - 3$ (Boss et al., 2001b,a). Assuming a hyperbolic PSD (Junge-type model), ξ describes the shape of the distribution: higher values of ξ indicate a steep distribution, in which smaller particles dominate. As the value of ξ decreases, the PSD becomes flatter, indicating an increasing abundance of larger sized particle and thus increasing mean particle size.

The two optical quantities, [chl]/c_p and $\tilde{b}_{bp}$, were used by Boss et al. (2004) to characterize suspended material in shallow coastal (Case II) waters. The study confirmed $\tilde{b}_{bp}$ to be an appropriate parameter for distinguishing particles with different composition. Moreover, a rough inverse relationship was found between $\tilde{b}_{bp}$ and [chl]/c_p. Since an increase in detritus (organic or inorganic material) results in higher values of c_p without affecting [chl], this ratio roughly indicates the abundance of phytoplankton relative to the total particle concentration. Presumably, the higher the value of [chl]/c_p,

the higher the phytoplankton contribution to the total particle composition, and therefore the lower the value of $\tilde{b}_{bp}$. For this reason, [chl]/c_p was proposed as an additional indicator for particle composition.

In this study we use the same optical quantities ($\tilde{b}_{bp}$ and [chl]/c_p) to characterize the suspended particles in the upper 200 m of the water column in oligotrophic, open ocean (Case I) waters. Few studies have focused on the vertical distribution of these properties to these depths in Case I waters (i.e. Twardowski et al., 2007), as most open ocean studies primarily investigate the spatial and temporal evolution of optical parameters in the very upper layer of the water column (i.e. Huot et al., 2008; Behrenfeld et al., 2005) due to its importance for remote sensing.

2 Background

The Hawaiian archipelago is located in the middle of the North Pacific subtropical gyre. This region is typically oligotrophic, with low nutrient concentrations in the euphotic zone. The low nutrient availability limits both phytoplankton biomass and primary productivity. The ecological community is typically dominated by small size phytoplankton (cyanobacteria and photosynthetic pico- and nanoeukariotes, (Campbell and Vaulot, 1993) and primary productivity is almost entirely sustained by recycled nutrients. Nutrient concentrations increase with depth within the seasonal thermocline, so that a deep chlorophyll maximum layer (DCML), characterized by concentrations between 0.2–0.4 mg Chl m^{-3}, typically occurs at the base of the mixed layer, at about 110–130 m depth (Falkowski et al., 1991).

Due to the interaction of prevailing Trade Winds with the mountains of the Hawaiian Islands of Maui and Hawaii, cyclonic and anticyclonic mesoscale eddies frequently evolve in the lee of the Big Island of Hawaii (Patzert, 1969; Lumpkin, 1998; Chavanne et al., 2002; Dickey et al., 2008). Cyclonic eddies are biologically "productive" and can induce large variations in the biogeochemical characteristics of oligotrophic regions (Falkowski et al., 1991; McGillicuddy et al., 1998; McNeil et al., 1999). These

eddies are characterized by a vertical uplift of the seasonal thermocline. Therefore these features display upwelling of deep, nutrient-rich waters into the euphotic zone. The increased nutrient availability can trigger an increase in primary productivity and a shift in the ecological community; thus cyclonic eddies are often characterized by phytoplankton blooms dominated by large size groups, such as diatoms.

The primary goal of the NSF-funded E-Flux project was to study the physical-biological interactions that occur within Hawaiian lee cyclonic eddies (Dickey et al., 2008). The third field experiment of the project (E-Flux III; 10–27 March, 2005; Benitez-Nelson et al., 2007; Dickey et al., 2008; Nencioli et al., 2008) focused on the cyclonic eddy, *Opal*, which was intensively sampled over a 3-week period. Figure 1 shows the location of the four stations where the vertical profiles analyzed in this study were collected. The estimated position of the center of the eddy at the time of data collection is also indicated in Fig. 1. Vertical sections of velocity (not shown, see Nencioli et al., 2008) clearly reveal the cyclonic (anticlockwise) circulation associated with the eddy. *Opal* was a well-developed cyclonic eddy, characterized by intense doming of isopycnal surfaces, and enhanced chlorophyll concentrations at its center (Fig. 2). The DCML shoaled from ≈120 to ≈70 m at the center of the eddy, where chlorophyll concentration reached its maximum values of ≈1 mg Chl m^{-3}.

Pigment and microscopy analyses of water samples collected during the third transect across the eddy center revealed that the phytoplankton bloom within *Opal* was characterized by a shift in the ecological community (Rii et al., 2008; Brown et al., 2008). The DCML at the center of the eddy was in fact dominated by large diatoms, which accounted for almost 85% of the total phytoplankton biomass at *Opal*'s core (Brown et al., 2008). Another important feature evidenced by microscopy analysis was the presence of a layer of "senescent" diatoms immediately above the "healthy" diatoms of the DCML at the center of the eddy. Up to 85% percent of the diatom frustules found in this layer were empty, lacking both chlorophyll and cytoplasm (Brown et al., 2008). At *Opal*'s core, the water column can therefore be divided into three different regions, each one characterized by different biogeochemical conditions and ecological commu-

BGD
6, 8075–8100, 2009

nities: (1) a surface mixed layer (0 to 40 m) still dominated by small phytoplankton; (2) the DCML (70 to 90 m) dominated by large, "healthy" diatoms; (3) and an intermediate layer between the two (40 to 70 m), characterized by high concentrations of empty frustules (Landry et al., 2008).

3 Instrumentation and methods

In-situ measurements of hydrographic and optical parameters were made with a ship deployed profiling package. Vertical profiles were performed at the four stations indicated in Fig. 1 down to a depth of ~450 m. A SeaBird Electronics 9/11+CTD was used to measure temperature, conductivity and depth. Chlorophyll concentrations and particle backscattering at 700 nm ($b_{bp}(700)$) were measured with a WET Labs ECO-FLNTU fluorometer/turbidity sensor. Hyperspectral absorption and attenuation coefficients were measured at 84 different wavelengths between 400 and 730 nm (resolution of ~4 nm) with a WET Labs AC-S. The measured coefficients included the contribution by all in-water constituents except water: $a_{pg}(\lambda)=a_p(\lambda)+a_g(\lambda)$, and $c_{pg}(\lambda)=c_p(\lambda)+a_g(\lambda)$, where a_p and c_p represents the absorption and total attenuation contributions due to particulate material and a_g is the absorption contribution to total beam attenuation coefficient due to dissolved material (scattering by dissolved material is assumed to be negligible, i.e. $b_g=0$). AC-S data were corrected for temperature and salinity effects using the coefficients derived by Sullivan et al. (2006). After this correction, the Zaneveld et al. (1994) proportional method was applied in order to correct for the scattering errors in the absorption measurements.

Values of the spectral slope of beam attenuation (γ) at different depths were computed from the c_p spectra using the relationship

$$c_p(\lambda) = A_c\lambda^{-\gamma} \quad (1)$$

where A_c is the amplitude of the spectrum, λ is wavelength and γ is the hyperbolic exponent (e.g. Boss et al., 2001b; Twardowski et al., 2001). Here we make the important

BGD
6, 8075–8100, 2009

assumption that the absorption due to dissolved material is negligible ($a_g(\lambda)\approx 0$), so that only particle attenuation contributes to the total attenuation, and $c_{pg}(\lambda)\approx c_p(\lambda)$. For Case I waters, the error introduced by this assumption is typically a small percentage of the observed value, especially in the surface mixed layer. Since measured attenuation coefficients at wavelengths >600 nm are small (comparable to the background noise), only wavelengths from 400 to 600 nm (a total of 54 wavelenghts) were used for the spectral fit of c_p. Once values of γ were computed, values of c_p at specific wavelengths could be obtained using Eq. (1). Following Boss et al. (2004), attenuation coefficients at 650 nm ($c_p(650)$) were used to compute [chl]/c_p.

We obtained $b_{bp}(700)$ by processing total instrument counts from the ECO-FLNTU sensor; however values were unreasonably high. The origin of the problem was most likely an inaccurate calibration, which resulted in an incorrect scale factor used to convert instruments counts into b_{bp}. In order to retrieve correct b_{bp} values from the FLNTU measurements, an alternative scaling factor was derived using the instrument counts at depths >400 m. Absorption and attenuation coefficients values measured at those depths are similar in magnitude to those observed in the Southeast Pacific ocean in extremely clear waters. In clear waters, the backscattering from pure seawater (b_{bsw}) accounts for 90 to 95% of the total backscattering (b_b), so that $b_b \approx 1.05\ b_{\mathrm{bsw}}$ (Twardowski et al., 2007). Using the method of Twardowski et al. (2007), based on the work of Morel (1974); Buiteveld et al. (1994), it was possible to derive values of b_{bsw} at 700 nm below 400 m from measured temperature and salinity data, and then b_b. Since both instrument counts and $b_b(700)$ were fairly constant below 400 m, the new scaling factor was simply computed as the average ratio between the two. FLNTU measurements were converted into $b_b(700)$ throughout the entire water column using the newly derived scaling factor. These values were then corrected by $b_{\mathrm{bsw}}(700)$ computed at each depth again, to obtain $b_{bp}(700)$. Assuming $a_p(700)\approx 0$ (e.g. Bricaud and Stramski, 1990; Babin and Stramski, 2002), $b_p(700)$ was simply equal to $c_p(700)$. The values of $b_p(700)$ and $b_{bp}(700)$ were used to derive $\tilde{b}_{bp}$.

All data were averaged using 0.5 m bins.

BGD
6, 8075–8100, 2009

4 Results

Figure 3 shows vertical profiles of chlorophyll concentration for the four stations from Fig. 1. All profiles are characterized by similar surface concentrations, a DCML, and a decrease in concentrations to values close to the fluorometer detection limit below the DCM. The distance of each sampling station from Opal's center varied (see Fig. 1), with Cast 35 being the furthest, and Cast 31 the closest. The four profiles display what is shown in the vertical section in Fig. 2, namely evidence of a shoaling of the DCML toward *Opal*'s core, which is in conformance with the isopycnal uplift associated with the eddy. At the same time, chlorophyll concentrations increase due to the higher nutrient availability in the euphotic zone. Photoadaptation also plays a role. Cast 35 shows a broad DCML at about 120 m depth, with chlorophyll concentrations up to 0.2 mg Chl m^{-3}. These conditions are typical for the Hawaiian region (e.g. Falkowski et al., 1991), so that Cast 35 can be considered representative of the background conditions outside the influence of *Opal*. On the other hand, Cast 31 can be assumed representative of the eddy-induced diatom bloom conditions. The DCML is located at about 70 m depth, 50 m shallower than in Cast 35. Chlorophyll concentrations show a 5-fold increase, reaching maximum values of the order of about 1 mg Chl m^{-3}, indicating the presence of a phytoplankton bloom at the center of the eddy. The DCML in Cast 31 is sharper than the one in Cast 35. Chlorophyll concentrations increase and decrease quite rapidly with depth, so that the layer of the DCML is characterized by chlorophyll concentrations >0.4 mg Chl m^{-3} only ~10 m thick.

Vertical plots of $c_p(650)$ are shown in Fig. 4. Surface values vary between 0.03 and 0.04 m^{-1}, whereas values at depth are very low for the four the casts. Similarly to the peaks in chlorophyll concentration in Fig. 3, the peaks in particle attenuation become shallower, and increase in magnitude towards *Opal*'s center. However, further comparison with Fig. 3 shows that for each profile the maximum value of $c_p(650)$ occurs a few meters above the DCML.

This is a common feature in oligotrophic regions (e.g. Kitchen and Zaneveld, 1990;

BGD
6, 8075–8100, 2009

Fennel and Boss, 2003; Boss et al., 2007). In fact, POC and chlorophyll maxima are regulated by different mechanisms: the former occur where phytoplankton grow rate is balanced by losses, whereas the latter are determined by photadaptation (i.e. the change of chlorophyll concentration per cell, in response to light level variations) and, to a lesser extent, by nutrient availability (Fennel and Boss, 2003).

The $c_p(650)$ profile from Cast 35 does not reveal any maximum associated with the DCML. Cast 31, on the other hand, is characterized by a $c_p(650)$ maximum broader than the corresponding peak in chlorophyll concentration. Both maxima quickly decay below 70 m, but the peak in particle attenuation extends to shallower depths (roughly up to 50 m). Since c_p is a good proxy for particle concentration, the broader peak can be attributed to the presence of the layer of "senescent" diatoms above the DCML at the center of Opal.

Figure 5 shows vertical plots of [chl]/c_p for Cast 35 and Cast 31 (the other two casts representing only intermediate conditions between these two). The profile from Cast 35 is characterized by constant values within the upper layer above 60 m, and a gradual increase between 60 m and 150 m depth. Cast 31 shows similar values in the upper layer above 50 m. Below that depth [chl]/c_p rapidly increases, reaching its maximum values between 80 and 110 m, and then it slowly decays.

The ratio between chlorophyll concentration and attenuation coefficient can vary depending on several factors. Among these, the proportion between mineral and living particles, the size distribution, photoadaptation, and phytoplankton composition are considered to be the most important (Boss et al., 2004). Since small size phytoplankton dominate the ecological community outside the eddy throughout the whole water column, the variation of [chl]/c_p with depth observed in Cast 35 is likely attributable to photadaptation. More specifically, the values increase with depth because chlorophyll concentration per cell increases as phytoplankton experience decreasing light levels. Interpretation of the profile from Cast 31 is more complex. The increase in [chl]/c_p between 50 and 70 m depths is most likely the result of both photoadaptation and pigment packaging associated with a change in phytoplankton composition from small phyto-

BGD
6, 8075–8100, 2009

plankton to diatoms. The broad maximum that occurs right below the DCML might result from another process serving as a controlling factor for [chl]/c_p: remineralization. It is possible that as phytoplankton are degraded or mineralized (this is consistent with the decreasing values of c_p(650) below the DCML), some of the chlorophyll might escape from broken cells into the water column in the form of chlorophyll and rapidly produced detrital phaeopigment. This might explain why chlorophyll fluorescence (including phaeopigment) remain much higher, despite lower c_p(650) values between 80 and 110 m compared to the values at the surface. For all four casts, vertical profiles of c_p(700) show similar features but slightly lower values than c_p(650) (not shown).

Profiles of b_{bp}(700) are shown in Fig. 6. The values at the surface are on the same order of magnitude as found by Huot et al. (2007), indicating that the method we developed to derive particle backscattering values from the ECO-FLNTU counts appears reasonable. The profile from Cast 31 resembles the chlorophyll profile, showing a sharp peak that reaches its maximum value at about 70 m depth. On the other hand, Cast 35 is more similar to the c_p(650) profile; b_{bp}(700) does not show a maximum occurring at the depth of the broad DCML.

Figure 7 shows the vertical profiles of $\tilde{b}_{bp}$ for Cast 31 and 35. Values at the surface are on the same order of magnitude of previous observations in the open ocean (Twardowski et al., 2007; Huot et al., 2008). The vertical profile for Cast 35 is characterized by roughly constant values of $\tilde{b}_{bp}$ down to a depth of ~60 m. Between 60 and 90 m depth, the ratio slowly increases, reaching slightly higher values between 90 and 120 m depth. The similar values between the two layers indicate that the particle population was dominated by small size phytoplankton, other water-filled organsims and detritus throughout the water column. The presence of small phytoplankton was confirmed by microscopic analysis. Nonetheless, the slightly higher values between 90 and 120 m depth might indicate a shift from surface to depth adapted species. Below 120 m, the backscattering ratio increases noticeably, indicating a shift toward smaller and/or possibly harder (i.e. higher bulk refractive index) material. This might be an indication of remineralization occurring below the DCML. The most important feature of the vertical

BGD
6, 8075–8100, 2009

profile from Cast 31 is the broad minimum between 50 and 70 m. This is related to the shift from small to large size phytoplankton observed at the center of the eddy, but may also be influenced by living cells with high relative water content (i.e., lower refractive index) being more dominant here relative to the surrounding water column. Even for this cast, the increase in values below the DCML can be interpreted as the result of phytoplankton degradation. This supports our hypothesis of remineralization being the main factor determining the broad maximum in [chl]/c_p below the DCML.

To further confirm that the minimum in $\tilde{b}_{bp}$ in Cast 31 reflects the observed shift in community at *Opal*'s core, the vertical profile of γ is plotted in Fig. 8. The values in the upper layer are comparable to the ones observed in previous studies (Twardowski et al., 2001; Boss et al., 2001b). As expected, between 50 and 70 m depth the profile shows a broad minimum. This indicates an increase in the mean particle size of the suspended material in that layer, and is compatible with the diatom-dominated phytoplankton bloom observed at the center of the eddy. As c_p becomes smaller with depth, our assumption that $c_{pg} \approx c_p$ is increasingly less valid. Even if only present in small concentrations, CDOM might have a larger contribution to the total attenuation at depth, because absorption spectra of CDOM are characterized by a hyperbolic slope of ≈ 7 (Twardowski et al., 2004). This might explain the high values of γ observed below 100 m depth.

5 Discussion and conclusions

The vertical distributions of the optical properties collected during the E-Flux III field experiment are clearly influenced by the presence of cyclone *Opal*. The isopycnal uplift and the phytoplankton bloom associated with the eddy result in a shoaling and an increase in magnitude of the peaks in chlorophyll concentration, $c_p(650)$ and $b_{bp}(700)$ from outside towards the center of the feature. The vertical profiles of chlorophyll and particle attenuation can be used to localize the depth range of the three ecological layers observed from the analysis of water samples. Near the center of the eddy, the

surface layer extends from the surface to 50 m depth, where both $c_p(650)$ and chlorophyll concentration begin to increase. The depth interval from 50 to 70 m is characterized by high concentrations of diatoms, as confirmed by the vertical profile of γ. This layer can be further divided into the "senescent" diatom layer and the DCML. The first extends from 50 to 60 m depth and is characterized by increasing chlorophyll concentrations, and a $c_p(650)$ value that has already reached its maximum. The second layer encompasses water depths of 60 to 70 m, where chlorophyll concentrations reach their maximum values.

According to our results, [chl]/c_p is not a good indicator for particle composition changes in the water column in Case I water, either in the case of background conditions, or in the presence of the eddy-induced phytoplankton bloom. The main factor controlling the variation of this ratio with depth is likely photoadaptation and not the bulk particle composition as observed in shallow coastal waters (Boss et al., 2004). Even in the presence of a diatom bloom as in Cast 31, the signal in [chl]/c_p resulting from the shift in ecological community is completely lost due to the large increase caused by photoadaption. Below the DCML remineralization might also be an important factor in regulating [chl]/c_p.

$\tilde{b}_{bp}$ is a better indicator for the bulk particle composition. It is nearly constant throughout Cast 35, indicating no variation in the ecological community outside the eddy. Its increase below the DCML is consistent with intense remineralization processes. For Cast 31, at the center of the eddy, $\tilde{b}_{bp}$ clearly indicates the position of the layer with increased diatom concentrations between 50 and 70 m depth. According to the $\tilde{b}_{bp}$ profile, the water column can be divided into three distinct layers: a surface layer with small size phytoplankton, a diatom-dominated middle layer, and a deep layer characterized by high remineralization. Unfortunately, it is not possible to further divide the middle layer into a "senescent" and a "healthy" diatom layer. The two layers do not seem to be characterized by distinct optical features, indicating some limitations on the information on particle composition that can be retrieved from optical measurements.

Finally, our data do not confirm the inverse relationship between $\tilde{b}_{bp}$ and [chl]/c_p

BGD
6, 8075–8100, 2009

found by Boss et al. (2004) for shallow coastal waters, either under background conditions, or during the eddy-induced phytoplankton bloom. This is particularly evident in Fig. 9. In these plots $\tilde{b}_{bp}$ is plotted against [chl]/c_p, combining information from both Figs. 5 and 7. The data shown in the two scatter plots are not binned and they are grouped into different depth intervals (color coded) depending on the different ecological communities. For Cast 35 (Fig. 9a), despite $\tilde{b}_{bp}$ remaining roughly constant down to ~120 m depth, [chl]/c_p steadily increases with depth. Since values of the backscattering ratio indicate the presence of a small size phytoplankton community throughout the whole water column, this confirms that the increase of [chl]/c_p reflects an increase in chlorophyll concentration per cell due to photoadaptaion. For Cast 31, Fig. 9b shows that the shift in community from small phytoplankton to diatoms below 50 m (evidenced by the minimum in $\tilde{b}_{bp}$), is characterized by an increase of [chl]/c_p as well. This is the only depth interval within which the two ratios show an inverse relationship. The variation in [chl]/c_p below 50 m depth might result from the change in community. Even if so, this variation cannot be distinguished from the increase in [chl]/c_p within the DCML induced by photoadaption. In both panels of Fig. 9, the increase observed in $\tilde{b}_{bp}$ within the deep layer while [chl]/c_p remains relatively high, reflects the enhanced remineralization processes occurring below the DCML.

This study shows that, despite some limitations, optical properties, and $\tilde{b}_{bp}$ in particular, can be successfully used to obtain information about the composition of the suspended particles in the water column in Case I waters. Knowledge of the vertical distribution of the suspended material from the analysis of collected water samples was crucial in order to couple the optical signature of a given depth interval to a specific biogeochemical state. However, the good correspondence between optical properties and the ecological structure within the water column, both inside and outside cyclone *Opal*, suggests that in the near future, with increasing number of experiments studying the relation between optical and biogeochemical characteristics under different conditions, continuous in situ optical measurements could be successfully used to obtain information on the bulk particle composition.

BGD
6, 8075–8100, 2009

Acknowledgements. Data used for this study were collected during the National Science Foundation (NSF) E-Flux experiment under a grant from the NSF Ocean Chemistry Program to Tommy Dickey. Dickey also received support from the NOPP MOSEAN project for the optical package, and his Secretary of the Navy/Chief of Naval Operation Chair in Oceanographic Science for his contribution to this paper. Funding for Francesco Nencioli was also provided by these grant. We thank all the E-Flux lproject collaborators for their intellectual contributions and sharing of ideas. Wil Black provided considerable assistance with the calibration of the optical instruments and the deployment of the profiling package. Casey Moore of WET Labs is thanked for his assistance and use of the optics package for this research.

References

Babin, M. and Stramski, D.: Light absorption by aquatic particles in the near-infrared spectral region, Limnol. Oceanogr, 47, 911–915, 2002. 8081

Behrenfeld, M., Boss, E., Siegel, D., and Shea, D.: Carbon-based ocean productivity and phytoplankton physiology from space, Global Biogeochem. Cy., 19, GB1006, doi:10.1029/2004GB002299, 2005. 8078

Benitez-Nelson, C., Bidigare, R. R., Dickey, T. D., Landry, M. R., Leonard, C. L., Brown, S. L., Nencioli, F., Rii, Y. M., Maiti, K., Becker, J. W., Bibby, T. S., Black, W., Cai, W. J., Carlson, C. A., Chen, F., Kuwahara, V. S., Mahaffey, C., McAndrew, P. M., Quay, P. D., Rappe, M. S., Selph, K. E., Simmons, M. P., and Yang, E. J.: Mesoscale eddies drive increased silica export in the subtropical Pacific Ocean, Science, 316, 1017–1020, 2007. 8079

boss2007 Boss, E. S., Collier, R., Larson, G., Fennel, K., and Pegau, W. S.: Measurements of spectral optical properties and their relation to biogeochemical variables and processes in Crater Lake, Crater Lake National Park, OR, Hydrobiologia, 547(1), 149–159, 2007.

Boss, E., Pegau, W., Gardner, W., Zaneveld, J., Barnard, A., Twardowski, M., Chang, G., and Dickey, T.: Spectral particulate attenuation and particle size distribution in the bottom boundary layer of a continental shelf, J. Geophys. Res., 106, 9509–9516, 2001a. 8077

Boss, E., Twardowski, M., and Herring, S.: Shape of the particulate beam attenuation spectrum and its inversion to obtain the shape of the particulate size distribution, Appl. Optics, 40, 4885–4893, 2001b. 8077, 8080, 8085

Boss, E., Pegau, W., Lee, M., Twardowski, M., Shybanov, E., Korotaev, G., and Baratange, F.:

Particulate backscattering ratio at LEO 15 and its use to study particle composition and distribution, J. Geophys. Res.-Oceans, 109, C01014, doi:10.1029/2002JC001514, 2004. 8077, 8081, 8083, 8086, 8087

Bricaud, A. and Stramski, D.: Spectral absorption-coefficients of living phytoplankton and non-algal biogenus matter – a comparison between the Peru upwelling area and the Sargasso Sea, Limnol. Oceanogr., 35, 562–582, 1990. 8081

Brown, S. L., Landry, M. R., and Selph, K. E.: Diatoms in the desert, Deep-Sea Res. II, 55, 1321–1333, 2008. 8079

Buiteveld, H., Hakvoort, J. H. M., and Donze, M.: The optical properties of pure water, in: SPIE Ocean Optics, 174–183, 1994. 8081

Campbell, L. and Vaulot, D.: Photosynthetic picoplankton community structure in the subtraopical North Pacific-Ocean near Hawaii (Station ALOHA), Deep-Sea Res. I, 40, 2043–2060, 1993. 8078

Chavanne, C., Flament, P., Lumpkin, R., Dousset, B., and Bentamy, A.: Scatterometer observations of wind variations induced by oceanic islands: Implications for wind-driven ocean circulation, Can. J. Remote Sens., 28(3), 466–474, 2002. 8078

Claustre, H., Bricaud, A., Babin, M., Bruyant, F., Guillou, L., Le Gall, F., Marie, D., and Partensky, F.: Diel variations in Prochlorococcus optical properties, Limnol. Oceanogr., 47, 1637–1647, 2002.

Dickey, T. D., Nencioli, F., Kuwahara, V. S., Leonard, C. L., Black, W., Bidigare, R. R., Rii, Y. M., and Zhang, Q.: Physical and bio-optical observations of oceanic cyclones west of the island of Hawai'i, Deep-Sea Res. II, 55, 1195–1217, 2008. 8078, 8079

Falkowski, P. G., Ziemann, D., Kolber, Z., and Bienfang, P. K.: Role of eddy pumping in enhancing primary production in the ocean, Nature, 352, 55–58, 1991. 8078, 8082

Fennel, K. and Boss, E.: Subsurface maxima of phytoplankton and chlorophyll: Steady-state solutions from a simple model, Limnol. Oceanogr., 48(4), 1521–1534, 2003.

Huot, Y., Babin, M., Bruyant, F., Grob, C., Twardowski, M. S., and Claustre, H.: Relationship between photosynthetic parameters and different proxies of phytoplankton biomass in the subtropical ocean, Biogeosciences, 4, 853–868, 2007, http://www.biogeosciences.net/4/853/2007/. 8084

Huot, Y., Morel, A., Twardowski, M. S., Stramski, D., and Reynolds, R. A.: Particle optical backscattering along a chlorophyll gradient in the upper layer of the eastern South Pacific Ocean, Biogeosciences, 5, 495–507, 2008,

http://www.biogeosciences.net/5/495/2008/. 8078, 8084
Kitchen, J.: On the noncorrelation of the vertical structure of light scattering and chlorophyll a in case I waters, J. Geophys. Res., 95(C11), 20237–20246, 1990.
Landry, M. R., Brown, K. E., Selph, K. E., Simmons, M. P., and Rii, Y. M.: Depth-stratified phytoplankton dynamics in Cyclone Opal, a subtropical mesoscale eddy, Deep-Sea Res. II, 55, 1348–1359, 2008. 8080
Lumpkin, C. F.: Eddies and currents in the Hawaii islands, Ph.d. thesis, University of Hawaii at Manoa, Honolulu, USA, 1998. 8078
McGillicuddy, D. J., Robinson, A. R., Siegel, D. A., Jannasch, H. W., Johnson, R., Dickey, T. D., McNeil, J. D., Michaels, A. F., and Knap, A. H.: Influence of mesoscale eddies on new production in the Sargasso Sea, Nature, 394, 263–266, 1998. 8078
McNeil, J. D., Jannasch, H. W., Dickey, T. D., McGillicuddy, D. J., Brzezinski, M., and Sakamoto, C. M.: New chemical, bio-optical and physical observations of upper ocean response to the passage of a mesoscale eddy off Bermuda, J. Geophys. Res., 104, 15537–15548, 1999. 8078
Morel, A.: Optical properties of pure water and pure seawater, Academic, New York, 1974. 8081
Morel, A.: Optical modeling of the upper ocean in relation to its biogenous matter content (Case I waters), J. Geophys. Res., 93(C9), 10749–10768, 1988. 8077
Nencioli, F., Kuwahara, V. S., Dickey, T. D., Rii, Y. M., and Bidigare, R. R.: Physical dynamics and biological implications of a mesoscale eddy in the lee of Hawai'i: Cyclone Opal observations during E-Flux III, Deep-Sea Res. II, 55, 1252–1274, 2008. 8079, 8093
Patzert, W. C.: Eddies in Hawaiian Islands, Report HIG-69-8, Hawaii Institute of Geophysics, University of Hawaii, Honolulu, USA, 1969. 8078
Rii, Y. M., Brown, S. L., Nencioli, F., Kuwahara, V. S., Dickey, T. D., Karl, D. M., and Bidigare, R. R.: The transient oasis: nutrient-phytoplankton dynamics and particle export in Hawaiian lee cyclones, Deep-Sea Res. II, 55, 1275–1290, 2008. 8079
Siegel, D. A., Dickey, T. D., Washburn, L., Hamilton, M. K., and Mitchell, B. G.: Optical determination of particulate abundance and production variations in the oligotrophic ocean, Deep-Sea Res. I, 36, 211–222, 1989. 8077
Sullivan, J., Twardowski, M., Zaneveld, J., Moore, C., Barnard, A., Donaghay, P., and Rhoades, B.: Hyperspectral temperature and salt dependencies of absorption by water and heavy water in the 400–750 nm spectral range, Appl. Optics, 45, 5294–5309, 2006. 8080

Twardowski, M., Boss, E., Macdonald, J., Pegau, W., Barnard, A., and Zaneveld, J.: A model for estimating bulk refractive index from the optical backscattering ratio and the implications for understanding particle composition in case I and case II waters, J. Geophys. Res.-Oceans, 106, 14129–14142, 2001. 8077, 8080, 8085

Twardowski, M. S., Claustre, H., Freeman, S. A., Stramski, D., and Huot, Y.: Optical backscattering properties of the "clearest" natural waters, Biogeosciences, 4, 1041–1058, 2007, http://www.biogeosciences.net/4/1041/2007/. 8078, 8081, 8084

Twardowski, M. S., Boss, E., Sullivan, J. M., and Donaghay, P. L.: Modeling the spectral shape of absorption by chromophoric dissolved organic matter, Mar. Chem., 89, 69–88, 2004. 8085

Zaneveld, J. R. V., Kitchen, J. C., and Moore, C. M.: The scattering error correction of reflecting tube absorption meters, in: Ocean Optics XII, 44–55, 1994. 8080

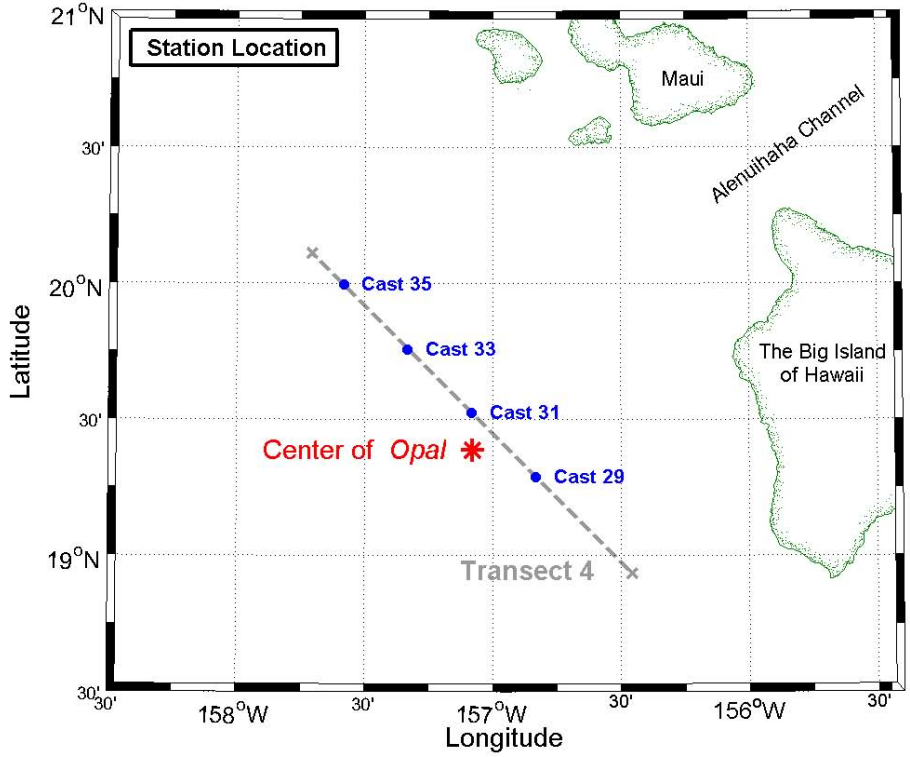

Fig. 1. Position of the four casts used in this study, and location of the estimated center of the eddy, *Opal*, at the time the casts were collected. The dashed line indicates the vertical section shown in Fig. 2.

BGD
6, 8075–8100, 2009

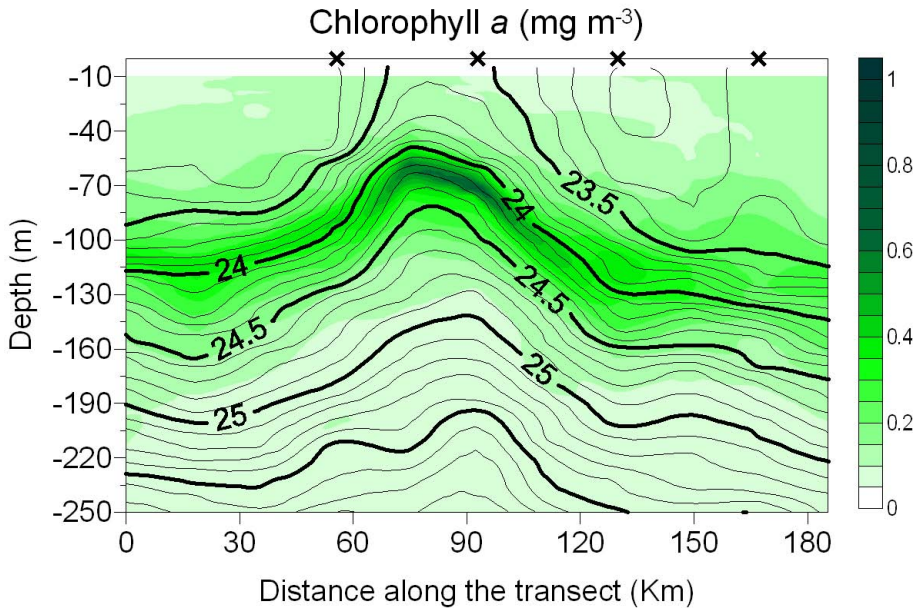

Fig. 2. Vertical section of chlorophyll concentration. The contourlines indicate isopycnal surfaces (σ_t values given). The black X's indicate the position along the transect of the four casts discussed in this study. The vertical section was reconstructed using all the vertical profiles available for the transect (see Nencioli et al., 2008).

BGD
6, 8075–8100, 2009

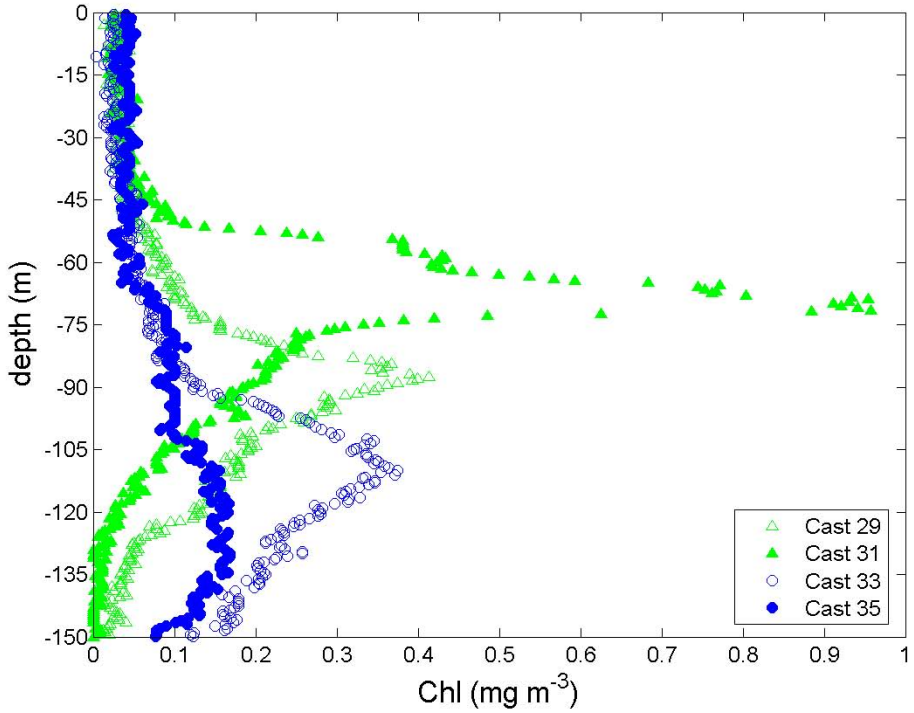

Fig. 3. Vertical profiles of chlorophyll concentration for the four casts.

BGD
6, 8075–8100, 2009

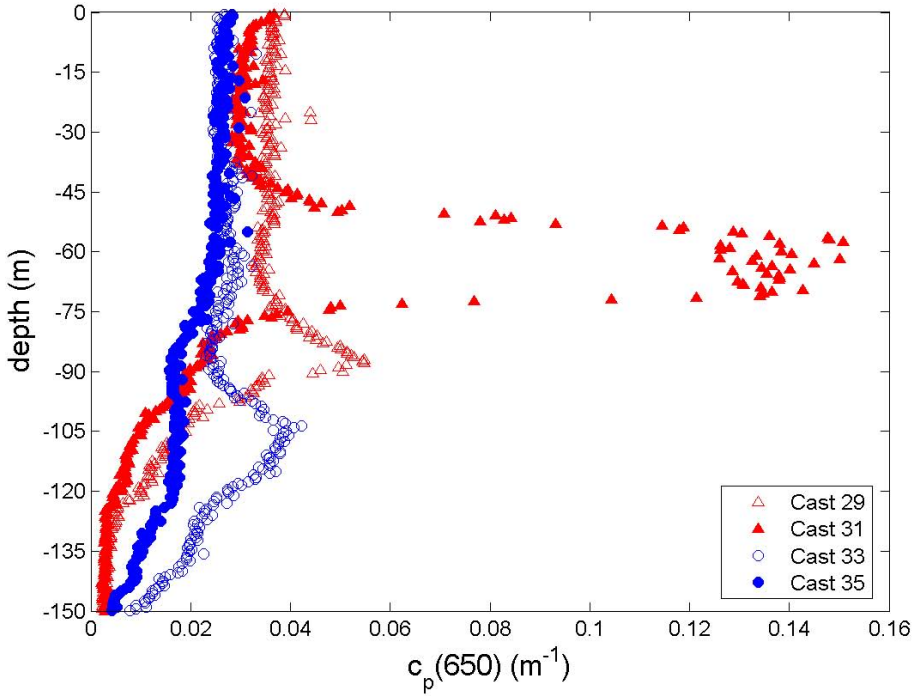

Fig. 4. Vertical profiles of attenuation coefficient for the four casts.

BGD
6, 8075–8100, 2009

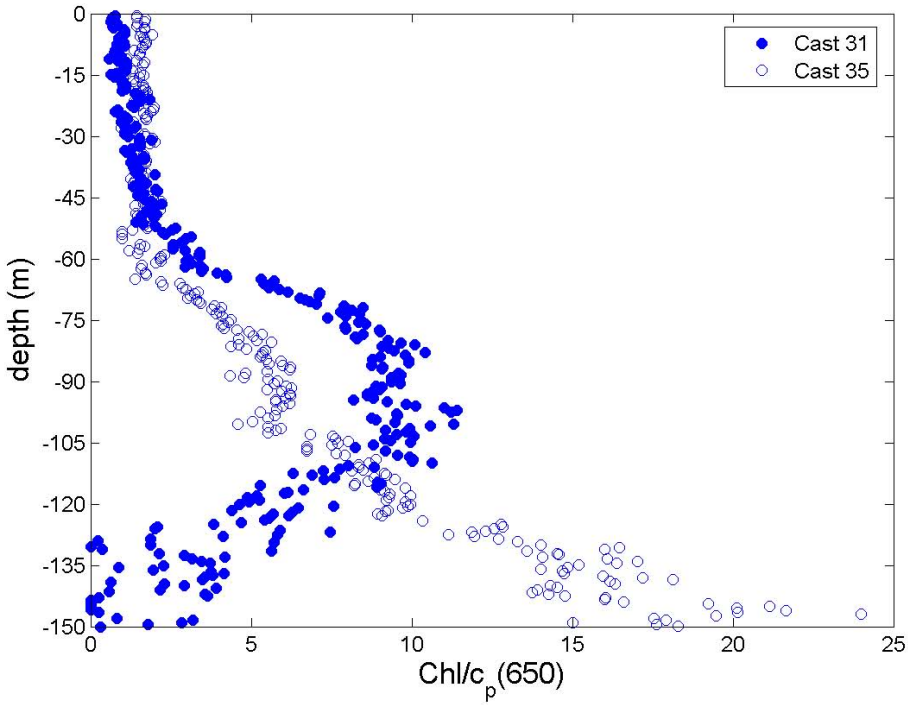

Fig. 5. Vertical profiles of [chl]/c_p for Cast 31 and 35.

BGD
6, 8075–8100, 2009

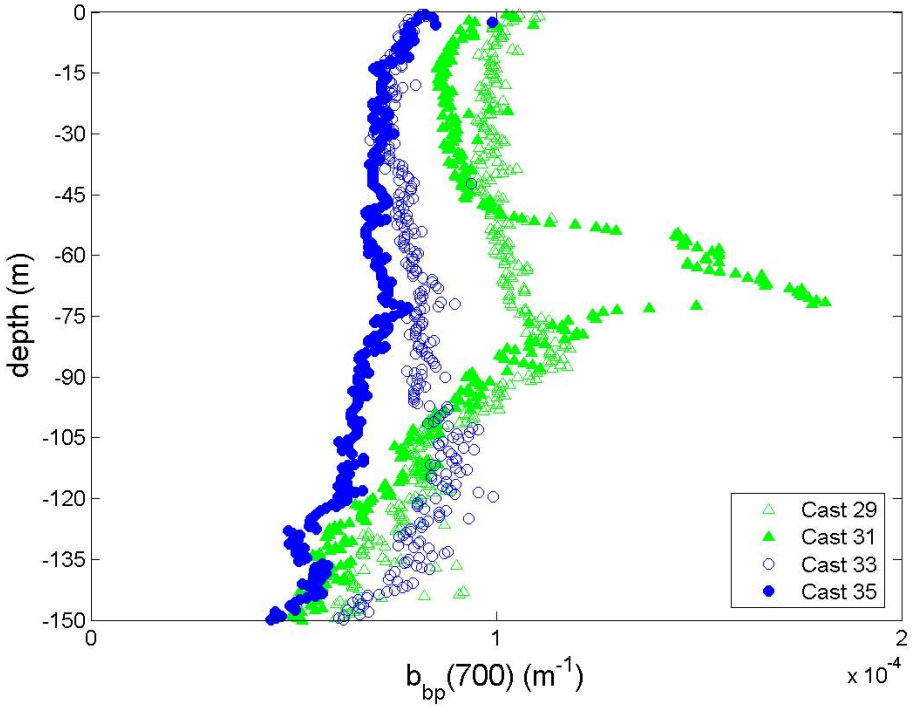

Fig. 6. Vertical profiles of $b_{bp}(700)$ for the four casts.

BGD
6, 8075–8100, 2009

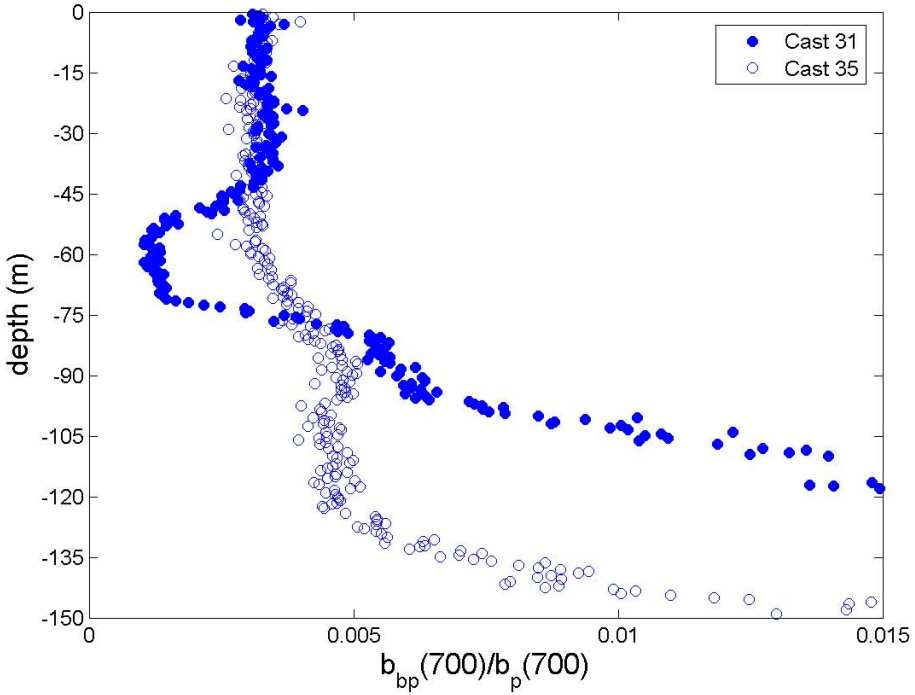

Fig. 7. Vertical profiles of $\tilde{b}_{bp}$ for Cast 31 and Cast 35.

BGD
6, 8075–8100, 2009

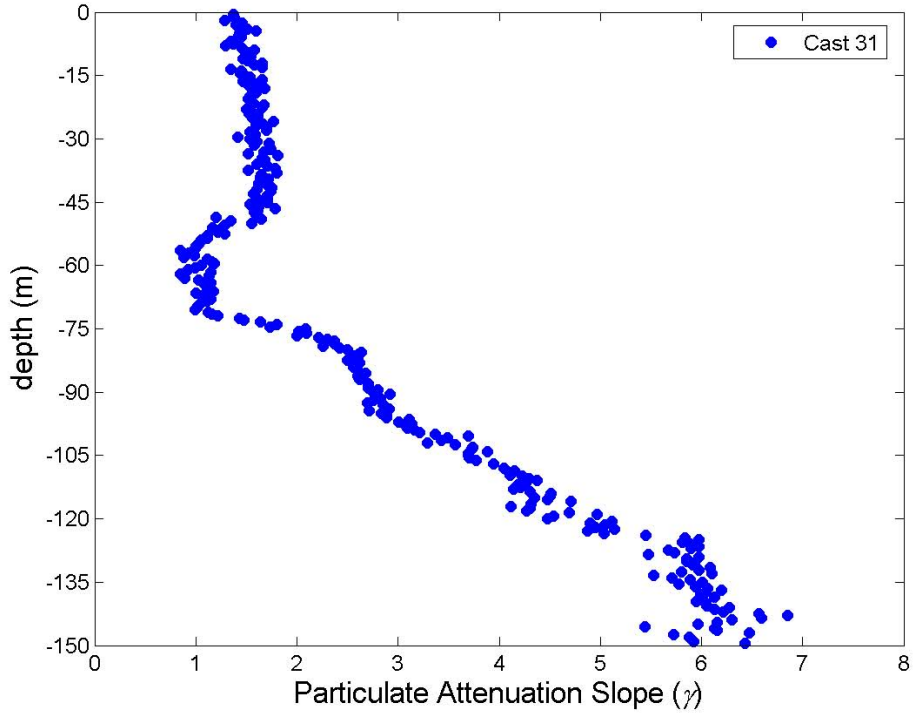

Fig. 8. Vertical profile of PSD slope (γ) for Cast 31.

BGD
6, 8075–8100, 2009

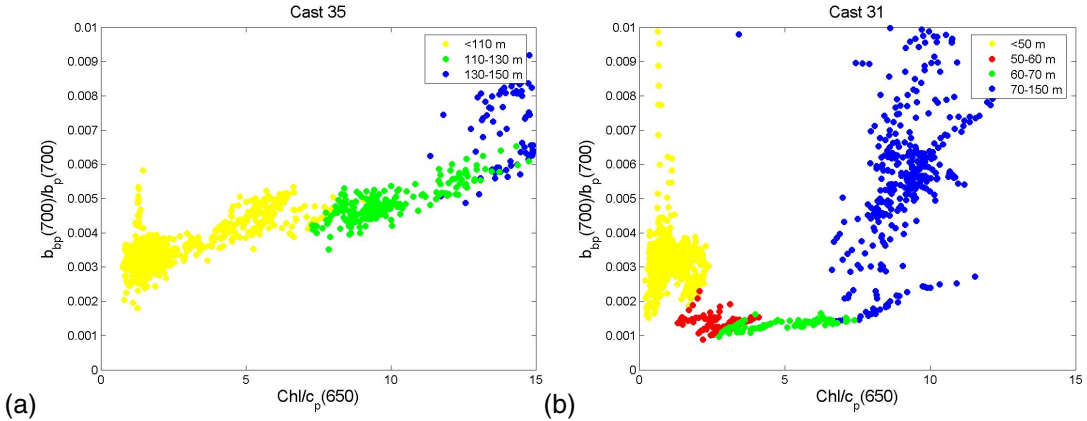

Fig. 9. Scatter plot of $\tilde{b}_{bp}$ versus [chl]/c_p for Casts 35 **(a)** and 31 **(b)**. The data shown are not binned, and they are grouped (using color coding) into four different depth intervals corresponding to distinct ecological communities.

BGD
6, 8075–8100, 2009